Available online at www.sciencedirect.com

ScienceDirect

Energy Procedia 124 (2017) 76–83

Energy Procedia

www.elsevier.com/locate/procedia

7th International Conference on Silicon Photovoltaics, SiliconPV 2017

Aspects of bifacial cell efficiency

Gaby J.M. Janssen*, Kees C.J. Tool, Eric J. Kossen, Bas B. Van Aken, Anna J. Carr, Ingrid G. Romijn

ECN-Solar Energy, Westerduinweg 3, 1755 LE Petten, The Netherlands

Abstract

This paper presents simulation and experimental results on the electrical response of n-PERT (passivated emitter rear totally diffused) solar cells under front and rear illumination. The so-called bifaciality factor, which represents the response to rear illumination compared to front illumination, is an important factor for determining the bifacial efficiency and predicting the annual energy output. This factor increased when the recombination parameters of the back-surface field and the base material were improved. Moreover, we found that the bifaciality factor of n-PERT cells increased strongly with the base resistivity. In simulations we studied the cell response under simultaneous front and rear side illumination. According to our results, the simulated bifacial efficiency agrees very well with the "compensated current" efficiency recently proposed for characterization of bifacial modules. The "compensated current" method therefore seems not only a convenient method for characterization of bifacial modules, but also very well suited for use in energy yield predictions.

Keywords: bifacial solar cells; baciality factor; bifacial efficiency; compensated current; energy yield prediction

1. Introduction

Because bifacial solar cells can convert light falling on the rear as well as on the front, they have a potentially higher energy yield. But since the lay-out of the cell is usually non-symmetrical, the response of the cell to light falling on the front or the rear is not the same. In other words, the bifaciality factor of the cell, defined as the ratio of the efficiency of the cell under rear illumination and under front illumination, is usually smaller than unity. Together

* Corresponding author. Tel.: +31 88 515 4803
E-mail address: janssen@ecn.nl

10.1016/j.egypro.2017.09.334

with a high front-side efficiency, a high bifaciality factor is needed to obtain optimal benefit from the two-side irradiance. As the bifaciality factor can be measured well with standard solar simulators using a non-reflective chuck, it is a convenient parameter to characterize bifacial cells [1]. In this paper we will first investigate how changes in the rear-side doping profile and the base-material properties can improve the bifaciality factor without deteriorating the front-side efficiency. For this we combine experimental and simulation studies.

But accurate estimates of the bifacial efficiency, and hence bifacial energy yield, cannot be made only from the front-side efficiency and bifaciality factor measured at 1 Sun illumination [2,3]. Therefore, with the use of simulations, we will look at a situation more realistic of a cell operating in the field, i.e. the cell under simultaneous front and rear illumination. In a laboratory, the characterization of a cell under such conditions is quite complicated, as sun simulators are usually designed for monofacial characterization [2]. We will compare the calculated bifacial efficiency to efficiencies calculated from parameters measured at 1 Sun such as the front-side efficiency and the bifaciality factor, and to efficiencies obtained by the so-called "compensated current" method [4]. This method, recently proposed to characterize bifacial modules, uses standard techniques for monofacial characterization but accounts for V_{OC} gains and FF losses that are due to the additional current generated by the rear illumination. These counteracting effects of V_{OC} and FF must be included in the characterization of bifacial cells and modules, as well as in the prediction of the bifacial energy yield.

2. The bifaciality factor

2.1 Experimental

We prepared n-PERT cells (n-Cz Si, 156x156 mm^2) with a diffused 60 Ω/sq front-side boron emitter according to the ECN n-Pasha process [5], using wafers with different resistivity (1, 2, 4.8, 5 and 9 Ω.cm). One set of cells had the standard back-surface field (BSF), the second set of cells had a more lightly doped BSF. SiN_x layers for antireflection and passivation were deposited on the front and on the rear side. The stencil-printed metallization on the front resulted in 4.4% metal coverage, at the rear the (screen-printed) metal coverage was 6.5%. The *I-V* measurements were conducted with a Class AAA solar simulator (Wacom) on a non-conductive, low reflective (anodized) chuck. Average measured front-side efficiencies were between 20.1 and 20.5% with standard and optimized BSF, respectively.

2.2 Simulations

We carried out simulations of the n-PERT cells with the Quokka code 2.2.4 [6]. For the passivated area of the emitter we assumed recombination parameter J_0 of 70 $fA.cm^{-2}$, for the contacted area 2500 $fA.cm^{-2}$. While the BSF contact J_0 was kept fixed at 1000 $fA.cm^{-2}$, the J_0 of the passivated part of the standard BSF was 160 $fA.cm^{-2}$, and 54 $fA.cm^{-2}$ for the optimized BSF. With an assumed bulk lifetime of 1 ms, the calculated front-side cell efficiency for the cell with standard BSF was 20.1-20.4 %, depending on the base resistivity. For the cells with optimized BSF the efficiency increased by 0.4 % absolute, confirming that assumed parametrization of the cells well reflects the cell properties.

2.3 Results and discussion

Of the cell *IV*-characteristics, i.e. the short circuit current J_{SC}, the open cell voltage V_{OC} and the fill factor FF, the J_{SC} is the most sensitive to which side of the cell is illuminated. Fig. 1 shows that the short-circuit current $J_{SC\text{-}rear}$ was lower than $J_{SC\text{-}front}$ and that this difference increased with decreasing base resistivity. Moreover, the effect was more pronounced for the cell with a standard BSF. The lower $J_{SC\text{-}rear}$ can in part be attributed to a larger rear metal coverage, 4.4 % and 6.5 % for front and rear respectively and optical properties. The remaining difference in $J_{SC\text{-}front}$ and $J_{SC\text{-}rear}$ is due to transport of charge carriers from the illuminated side to the other side of the cell, where they are collected.

In a cell with a front-side emitter and under front-side illumination, the charge carrier transport to the rear (BSF side) is field-driven transport of majority charge carriers. Upon rear illumination minority charge carriers have to travel from the BSF through the base to the emitter. This transport is diffusion driven, and therefore a high concentration of excess carriers Δn builds up near the BSF. This results in enhanced BSF recombination. At the diffused BSF with a recombination parameter $J_{0,BSF}$, the total associated recombination current can be written as:

$$J_r = J_{0,BSF} \frac{\Delta n \cdot (N_D + \Delta n)}{n_i^2} \quad (1)$$

Here N_D is the doping of the wafer. At short-circuit conditions (SC), the doping concentration is essentially the concentration of the majority charge carriers ($\Delta n << N_D$). The minority carrier concentration Δn is at SC first of all determined by the illumination level. As a lower base resistivity corresponds to a higher doping concentration ($N_D \sim 1/\rho$), the recombination increases with decreasing resistivity. A reduction of the recombination parameter $J_{0,BSF}$ will, according to eq. 1, not only reduce the total recombination but also the dependency on the base resistivity. This is confirmed by the results in Fig. 1 where the $J_{0,BSF}$ of the optimized BSF was 100 fA.cm^{-2} lower than of the standard BSF.

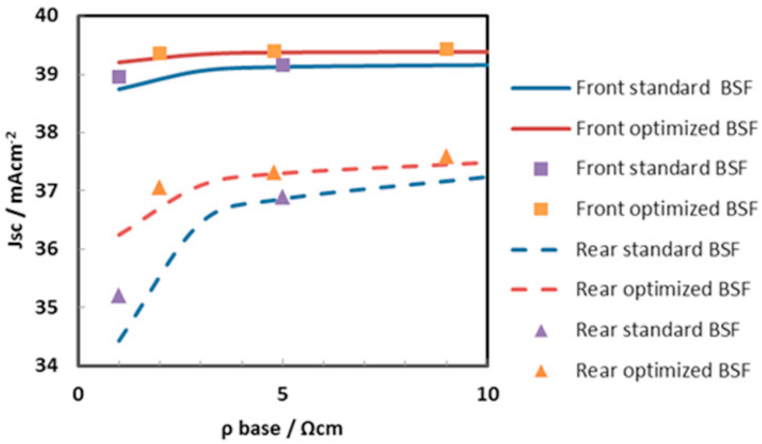

Fig. 1. Simulated (lines) and measured (points) J_{SC} values of n-PERT cells as function of base resistivity ρ, at 1 Sun front or 1 Sun rear illumination. This figure compares the standard BSF and the optimized BSF.

The ratio of V_{OC} or the front and rear FF differed from unity by maximum 0.6% only. As a result of the similar front and rear V_{OC} and FF, the bifaciality factor for the efficiency ($\eta_{rear} / \eta_{front}$) is essentially equal to the bifaciality factor of the J_{SC}, i.e. $J_{SC\text{-}rear}/ J_{SC\text{-}front}$, as demonstrated in Fig. 2. Optimization of the BSF in our n-PERT cells resulted in not only an increase of V_{OC} from 653 mV to 666 mV, but also a higher, less base-resistivity dependent bifaciality factor.

It is not so surprising that the V_{OC} is not dependent on the illumination side, but for FF the explanation is less straightforward. At open circuit the excess carrier distribution is not transport determined but recombination determined, and therefore only slightly dependent on the illumination side. However, the resistive losses in the cell at maximum power point (MPP) have a large impact on the fill factor, and they are expected to be smaller for field-driven majority transport than for diffusion-driven minority transport. An in-depth study of the effects of front or rear illumination on the FF is beyond the scope of this work, but we want to point out that the calculated pFF values were not really different for front or rear illumination. This was expected as the pFF essentially reflects open-circuit conditions. However, the free-energy loss analysis of the Quokka simulations also showed that the resistive losses at MPP were 1-1.5 mW.cm^{-2} higher at 1 Sun rear illumination than at 1 Sun front illumination. Although the resistive losses are often equated to $J_{SC} \cdot V_{OC} \cdot (pFF\text{-}FF)$, they are in fact part of the difference between the pseudo power $J_{gen} \cdot V_{OC} \cdot pFF$ and the actual power $J_{SC} \cdot V_{OC} \cdot FF$. As the difference between the generated current J_{gen} and the J_{SC} is larger for the rear than for the front, the higher resistive losses under rear illumination do not necessarily result in a lower FF.

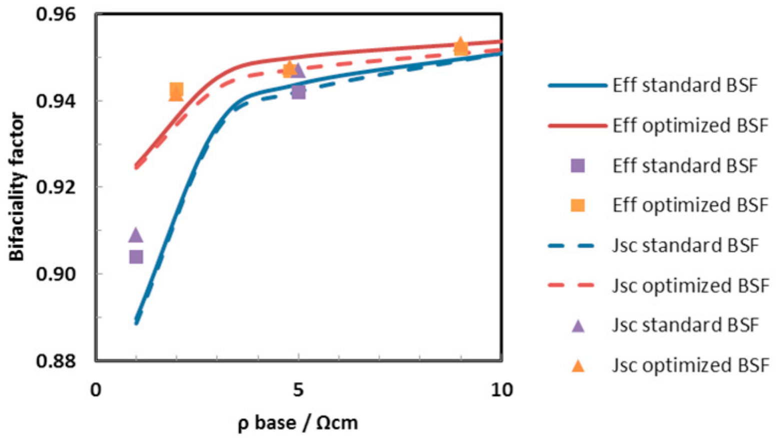

Fig. 2. Simulated (lines) and measured (points) of the bifaciality factor of n-PERT cells as function of base resistivity ρ. The figure shows the bifaciality factor for the J_{SC} as well as for the efficiency, and compares the standard BSF and the optimized BSF.

The higher Δn in the base associated with rear-side illumination means that improvement of the base lifetime has a stronger impact on the rear J_{SC} than on the front J_{SC}, as Fig. 3 shows, However, since the base Shockley-Read-Hall (SRH) recombination is in first order independent of the base doping, this effect does not vary with the resistivity.

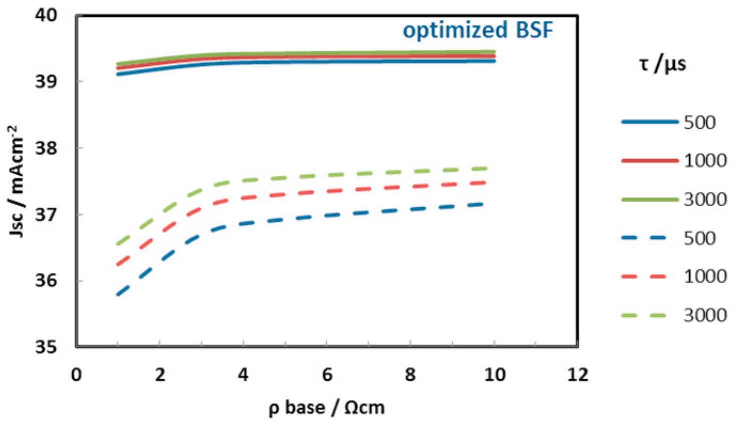

Fig. 3. Simulated $J_{SC\text{-}front}$ (solid lines) and $J_{SC\text{-}rear}$ (dotted lines) of n-PERT cell with an optimized BSF as function of base resistivity ρ. The base lifetime τ was varied.

Since at SC the recombination current is proportional to Δn and since the generated current J_{gen} as well as Δn at SC are proportional to the illumination level, the J_{SC} will both for front and rear be proportional to the illumination level. It is therefore predicted and confirmed by simulations that the bifaciality factor is in first order independent of the illumination level (Fig. 4).

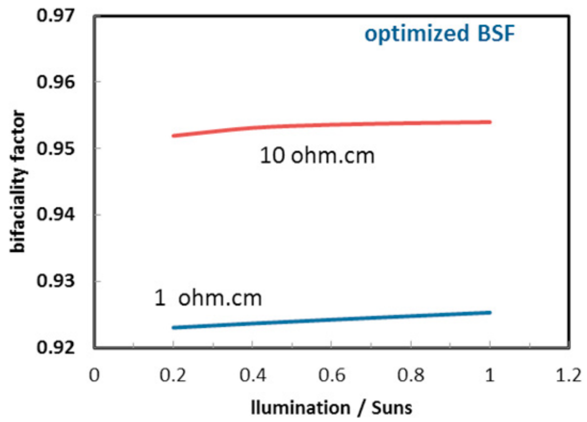

Fig. 4. Bifaciality factor for the efficiency as function of illumination level for n-PERT cells with an optimized BSF at two values of the base resistivity ρ.

3. Simultaneous illumination on front and rear side

3.1 Simulations

The Atlas package from Silvaco has the option to use simultaneous front and rear illumination [7]. We considered two cases of illumination:

A: 1 Sun front + x Sun rear
B: (1-x) Sun front + x Sun rear

Case A is reflective of an equator-facing system where the most of the day the front illumination will dominate and the rear makes an additional contribution. Case B more resembles the east-west facing systems where, at a given moment during the day, either side can receive the larger illumination but the maximum illumination per side will be about the same. The simulated cells differed in some aspects from the cells in the previous section, with front-side efficiencies between 21 and 21.5%, depending on the base resistivity. The bifaciality factors for the efficiency were 0.92, 0.95 and 0.97 at base resistivity 1, 2.7 and 10 ohm.cm, respectively.

3.2 Results and discussion

Having only a front and rear side characterization of a bifacial cell available, a very simple approach to predict the bifacial J_{SC} would be a linear combination of the front and rear J_{SC} at 1 Sun weighed by the respective illuminations. This means that for case A described above:

$$J_{SC-bif} = J_{SC-front} + x\, J_{SC-rear} \quad (2a)$$

and for case B:

$$J_{SC-bif} = (1-x)\, J_{SC-front} + x\, J_{SC-rear} \quad (2b)$$

Fig. 5 shows that, all at base-resistivity values considered, there is very good agreement between the bifacial J_{SC} obtained from simulations and the simple linear combination of the $J_{SC\text{-}front}$ and $J_{SC\text{-}rear}$. The main cause of this good agreement is, of course, that the J_{SC} is to a good order proportional to the illumination level.

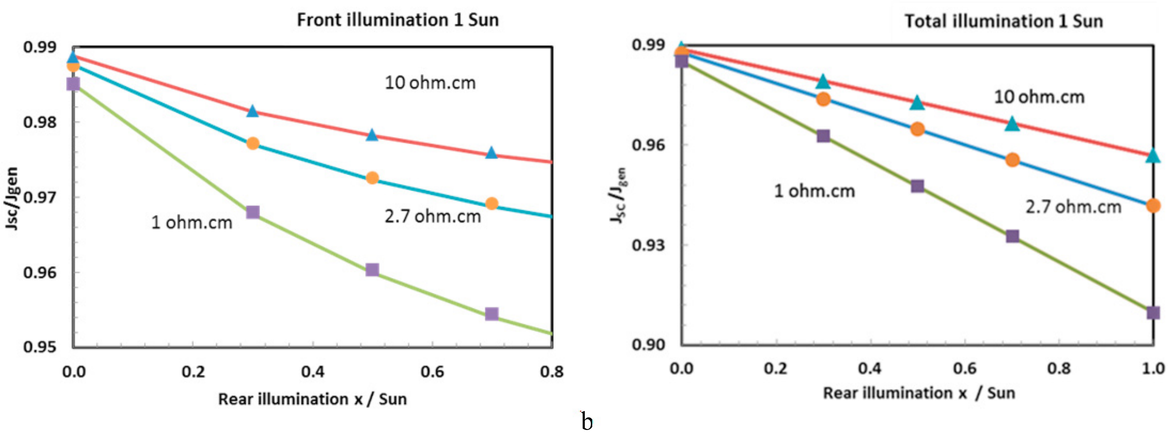

a b

Fig. 5. (a) Simulated bifacial J_{SC} (points) and approximated J_{SC} (lines) for Case A according to eq. 2a; (b) for Case B according to eq. 2b. To make the difference between J_{SC} at different base resistivity more clear, Fig. 5 shows the total J_{SC} scaled by the total generation current J_{gen} (which is 40.4 mA.cm^{-2} in Fig. 5b and increases from 40.4 mA.cm^{-2} at x=0 to 80.8 mA.cm^{-2} at x=1 in Fig. 5a).

Using eq. 2a and 2b, and the observation that V_{OC} and FF do not depend on the illumination side, in the calculation of the power output $P(x)$ we would obtain

for case A: $$P(x) = \left(J_{SC-front} + x\, J_{SC-rear}\right) \cdot V_{OC}(1+x) \cdot FF(1+x) \quad (3a)$$

for case B: $$P(x) = \left((1-x)\, J_{SC-front} + x\, J_{SC-rear}\right) \cdot V_{OC}(1) \cdot FF(1) \quad (3b)$$

If $V_{OC}{\cdot}FF$ were independent of x, it would be possible to rewrite the equations as:

for case A: $$P(x) = \left(1 + x\, f_{bif}\right) \cdot P_{front} \quad (4a)$$

for case B: $$P(x) = \left(1 - x\left(1 - f_{bif}\right)\right) \cdot P_{front} \quad (4b)$$

In these equations f_{bif} is the bifaciality factor for the J_{SC} and P_{front} the front-side power output at 1 Sun (1000 Wm^{-2}), respectively. However, as the results presented in Fig. 6 confirm, the approximation according to eq. 4a-4b is only valid for case B. For case A, the V_{OC} will increase and the FF will decrease with increasing x, i.e. increasing total illumination. Although the effects are counteracting, the product $V_{OC}{\cdot}FF$ will not be constant when the total illumination changes. As already shown in section 2, the product $V_{OC}{\cdot}FF$ is quite similar for 1 Sun front illumination and 1 Sun rear illumination. Therefore, it is not surprising that for case B the simple relation of eq. 4b is a good approximation, especially when bifaciality factor for the efficiency is used.

To overcome the shortcomings of the above approximation, recently the so-called "compensated current" method was proposed to measure the bifacial efficiency of modules [3]. This method allows for the change of V_{OC} and FF with total illumination, but retains the simplicity of monofacial characterization. In this method, the contribution of the rear illumination, scaled by the bifaciality factor f_{bif}, is added to the front. The effective front side illumination G would for case A and B amount to:

A: $$G(x) = 1 + x\, f_{bif} \quad (5a)$$

B: $$G(x) = 1 - x + x\, f_{bif} \quad (5b)$$

In both cases *G(x)* is expressed in Suns. In the "compensated current" method f_{bif} is the bifacial factor for the efficiency. i.e. any small differences in $V_{OC}{\cdot}FF$ upon 1 Sun front or rear illumination are accounted for. The power output measured with front-side illumination *G(x)* is then considered as the bifacial power output at the illumination conditions with *x* Sun rear illumination. We applied the same method in cell simulations and compared it to simulations with true bifacial illumination. Fig. 6 shows that the "compensated current" method gives a very good representation of the bifacial power output.

Given the results presented here, we can conclude that the compensated current works so well because it accounts for the change in $FF{\cdot}V_{OC}$ when the total current changes and because it includes the different response of the *Jsc* to front and rear illumination through the bifaciality factor. Note, that an underlying assumption of the "compensated current" method is that the bifaciality factor is independent of the illumination level, i.e. the factor measured at 1 Sun is applicable for the whole range of rear illumination levels. This independency is corroborated by the results in section 2. The "compensated current" can also be very useful in predictions of the energy yield of bifacial systems as it requires only a modification of the illumination level fed to the monofacial electrical model.

Recently, Singh et al. proposed a method to predict the bifacial efficiency based on the front and rear characterization at 1 Sun [2]. Obviously*,* the "compensated current" method requires more measurements. The method of Sing et al., on the other hand, involves a rather complicated estimation of the resistive losses based on *FF* and *pFF* data. As mentioned in section 2, this approach may introduce errors. The "compensated current" method seems to give more straightforward information of the bifacial efficiency.

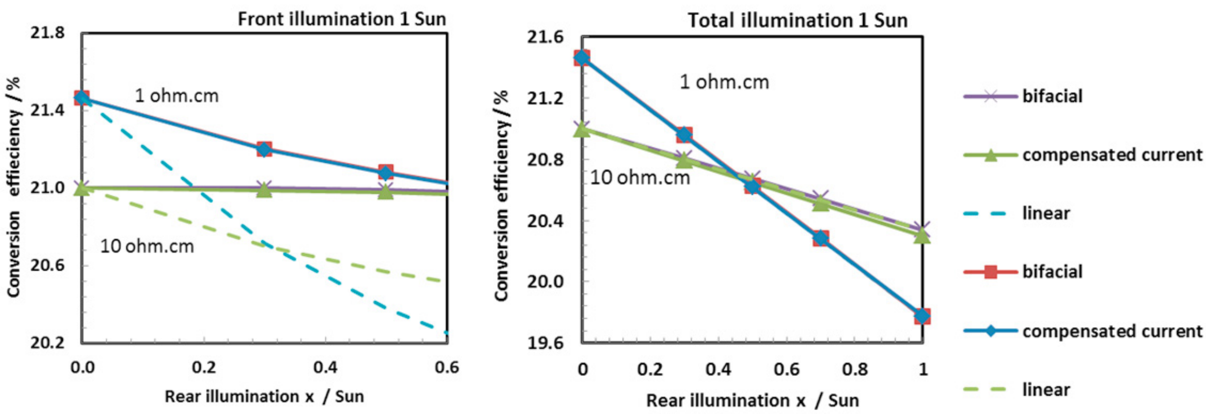

a b

Fig. 6. (a) The bifacial conversion efficiency for Case A calculated from simulations, the compensated current method (eq. 5a) and the linear approximation from eq. 4a. ; (b) for Case B using eq. 5b and 4b. For clarity the conversion efficiency rather than the power output is shown. This means that in Fig. 6a the bifacial power output was divided by the total irradiance (1+x) Sun. In Fig. 6b the conversion efficiency was calculated by dividing the power output by 1 Sun.

4. Conclusions

Both from experiments and from simulations we found that the response of an n-PERT cell to front or rear illumination, reflected in the bifaciality factor, can be very different and that this difference depends on the base-resistivity and BSF doping. The bifaciality factor is mainly determined by a different J_{SC} under front or rear illumination. By improving the BSF recombination properties, it is possible to increase the bifaciality factor and make it less dependent on the base resistivity. The bifaciality factor also increases when the base life-time improves, but this increase is independent of the base resistivity. Our simulations showed only a weak dependence of the bifaciality factor on the illumination level.

Although it seems that the current of a bifacial system can be well estimated from the front and rear J_{SC} measured at 1 Sun conditions, a simple prediction of the bifacial power output or efficiency from monofacial 1 Sun measurements is not possible. However, according to simulations the recently proposed “compensated current” method is a good approximation to the bifacial power output and efficiency, and can be used for experimental characterization as well as in yield prediction calculations.

References

[1] Kopecek R, Vishkasougheh MH, Gerritsen E, Schneider A, Comparotto C, Mihailetchi VD, Lossen J, Libal J. Bifaciality: One small step for technology, one giant leap for kWh cost reduction. Photovoltaics International 2014;26:32-45.

[2] Singh JP, Aberle AG, Walsh TM. Electrical characterization method for bifacial photovoltaic modules. Solar Energy Materials and Solar Cells 2014;127:136-42.

[3] Singh JP, Walsh TM, Aberle AG. A new method to characterize bifacial solar cells. Prog.Photovolt: Res.Appl. 2014;22:903-9.

[4] Electric Power Research Institute EPRI, Bifacial Solar Photovoltaic Modules - Program on Technology Innovation; 2016.

[5] Romijn IG, van Aken BB, Barton PC, Gutjahr A, Komatsu Y, Koppes M, Kossen E, Lamers MWPE, Saynova DS, Tool CJJ, Zhang Y. Industrial cost effective N-PASHA solar cells with >20% efficiency . 28th EUPVSEC, Paris; 2013.

[6] Fell A. A Free and Fast Three-Dimensional/Two-Dimensional Solar Cell Simulator Featuring Conductive Boundary and Quasi-Neutrality Approximations. IEEE Transactions on Electric Devices 2013;60:733-8.

[7] Atlas, Silvaco Inc, Sta Clara, Ca, www.silvaco.com.